Molecular Pathogenesis of Genetic and Inherited Diseases

Mutation of δ-Sarcoglycan Is Associated with Ca^{2+}-Dependent Vascular Remodeling in the Syrian Hamster

Larissa Lipskaia,* Caroline Pinet,* Yves Fromes,[†]
Stéphane Hatem,* Isabelle Cantaloube,*
Alain Coulombe,* and Anne-Marie Lompré*

*From INSERM U621, Université Pierre et Marie Curie-Paris6,
Unité Mixte de Recherche (UMR) S621,* Paris; and INSERM
U582, Institut de Myologie, Université Pierre et Marie Curie-
Paris6, UMR S582, Groupe Hospitalier Paris Saint Joseph,
Servicede Chirurgie Cardiaque,[†] Paris, France*

**We examined whether mutation of the δ-sarcoglycan
gene, which causes dilated cardiomyopathy, also al-
ters the vascular smooth muscle cell (VSMC) pheno-
type and arterial function in the Syrian hamster CHF
147. Thoracic aorta media thickness showed marked
variability in diseased hamsters with zones of atrophy
and hypertrophied segments. CHF-147 VSMCs dis-
played a proliferating/"synthetic" phenotype charac-
terized by the absence of the smooth muscle myosin
heavy chain SM2, dystrophin, and Ca^{2+}-handling
proteins, and the presence of cyclin D1. In freshly
isolated VSMCs from CHF 147 hamsters, voltage-inde-
pendent basal Ca^{2+} channels showed enhanced activ-
ity similar to that in proliferating wild-type (WT) cells.
The transcription factor NFAT (nuclear factor of acti-
vated T cells) was spontaneously active in freshly
isolated CHF 147 VSMCs, as in proliferating VSMCs
from WT hamsters. Mibefradil inhibited B-type chan-
nels, NFAT activity, and VSMC proliferation. CHF 147
hamsters had abundant apoptotic cells distributed in
patches along the aorta, and clusters of inactive mito-
chondria were observed in 25% of isolated CHF 147
cells, whereas no such clusters were seen in WT cells. In
conclusion, mutation of the δ-sarcoglycan gene in-
creases plasma membrane permeability to Ca^{2+}, acti-
vates the Ca^{2+}-regulated transcription factor NFAT, and
leads to spontaneous mitochondrial aggregation, caus-
ing abnormal VSMC proliferation and apoptosis.** *(Am J
Pathol 2007, 171:162–171; DOI: 10.2353/ajpath.2007.070054)*

Disruption of the plasma membrane-associated sarcogly-
can-sarcospan complex as a result of genetic defects causes muscular dystrophy and/or cardiomyopathy in hu-
mans (limb-girdle muscular dystrophy).[1] There are six sar-
coglycan family members: α-, β-, γ-, δ-, ε-, and ζ-sarcogly-
can.[2] In hamster and mouse models, δ-sarcoglycan gene
deletion results in myopathy of cardiac and skeletal mus-
cles, with focal areas of necrosis[3–5] and autophagic cardi-
omyocyte death.[6] Most of the studies on δ-sarcoglycan-
deficient animals have been conducted on skeletal and
cardiac muscles. The few studies on smooth muscle con-
cerned the vasospasm of coronary arteries, but there are no
data on the peripheral vessels. Sarcoglycans are trans-
membrane components of the dystrophin-glycoprotein
complex, which links the cytoskeleton to the extracellular
matrix.[7] At the cellular level, disruption of the dystrophin-
glycoprotein complex leads to increased permeability to
divalent cations through channel-blocker-sensitive path-
ways and entry of calcium via nonspecific cation chan-
nels.[8–11] The mechanisms of this enhanced Ca^{2+} influx are
not fully understood, but changes in the activity of several
Ca^{2+} channels have been described in dystrophin-defi-
cient myocytes.[12–15] Dystrophin, through PDZ domain-con-
taining adaptor proteins known as syntrophins, can link the
cytoskeleton to various membrane proteins carrying a PDZ
domain, including ion channels.[16] This cytoskeleton-ion
channel interaction contributes to receptor/channel local-
ization and to the regulation of voltage-, ligand-, and store-
operated ion channels. Indeed, restoration of functional
dystrophin-sarcoglycan complex formation by gene trans-
fer of minidystrophin or δ-sarcoglycan normalizes ion chan-
nel function in dystrophic myocytes.[10,12,17,18]

In vascular smooth muscle cells (VSMCs), Ca^{2+} ho-
meostasis not only controls vessel tone but also defines
the cell phenotype (from quiescent/contractile to prolifer-
ating/"synthetic"). The proliferating/synthetic phenotype

is associated with a reduction in contractile performance owing to the loss of adult isoforms of contractile proteins and dystrophin.[19] Moreover, proliferating VSMCs lose RyR and sarco(endo)plasmic reticulum Ca^{2+} ATPase (SERCA) 2a,[20] LTCC (L-type Ca^{2+} channels) are replaced by TTCC (T-type Ca^{2+} channels), and SOC (store-operated channels) as well as TRPCs (transient receptor potential protein family C) are up-regulated.[21] This results in an increased cytosolic Ca^{2+} concentration and changes in the spatiotemporal pattern of Ca^{2+} signals, which can alter gene expression by activating various protein kinases and phosphatases and Ca^{2+}-sensitive transcription factors.[22,23] For instance, a sustained increase in cytosolic Ca^{2+} is necessary to activate calcineurin, a Ca^{2+}/calmodulin-dependent serine/threonine-specific protein phosphatase 2B (PP2B) that dephosphorylates nuclear factor of activated T cells (NFAT), inducing its translocation into the nucleus and transcriptional activation. NFAT is involved in the control of cell cycle-related proteins required for VSMC proliferation[24,25]

The aim of this study was to determine the consequences of δ-sarcoglycan gene mutation on vessels of CHF 147 myopathic Syrian hamsters. We postulated that alterations of the dystrophin/sarcoglycan complex would be associated with enhanced transmembrane Ca^{2+} influx and with activation of Ca^{2+}-dependent processes in VSMCs.

Materials and Methods

Animals

Animals were treated in accordance with institutional guidelines. The study was performed on thoracic aortas from 6- to 12-month-old male and female cardiomyopathic Syrian hamsters of the strain CHF 147 (raised by INSERM U582, Paris, France) and their control Golden hamsters (WT) obtained from Janvier-France breeders.

Materials

All media, sera, and antibiotics were from Invitrogen (Cergy Pontoise, France). All chemicals were from Sigma-Aldrich (Saint Quentin Fallavier, France). The following primary antibodies were used: anti-SERCA 2a and anti-SERCA 2b (provided by Dr. F. Wuytack, University of Leuven, Leuven, Belgium),[26] anti-RyR (provided by I. Marty, INSERM U607, Département Réponse et Dynamique Cellulaires-Grenoble, France),[27] anti-SM2 (Ab 683; Abcam plc, Cambridge, UK), anti-NM-MHC-B (Ab 684; Abcam), anti-dystrophin (NCL-DYS2; Novocastra, Newcastle, UK), anti-caveolin 1 (ab2910; Abcam), anti-PMCA (ab2825; Abcam), anti-cyclin D1 (556470; BD Biosciences), and anti-NFATc1 (K-18; Santa Cruz Biotechnology, Santa Cruz, CA).

Histology and Immunofluorescence Studies

Media thickness was measured on hematoxylin and eosin-stained frozen cross sections with a computer-based morphometric system (Lucia; Nikon, Tokyo, Japan). Ten measurements were made on each section, and five discontinuous sections were analyzed in each animal. Ten CHF 147 and 10 WT hamsters were studied.

Apoptosis was analyzed by terminal deoxynucleotidyl transferase dUTP nick-end labeling staining of fixed cross sections with a standard protocol (ApopTag Red; Serologicals Corporation, Norcross, GA). Immunocytochemical analysis was applied to methanol-fixed cells or acetone-fixed sections according to a standard protocol (Santa Cruz Biotechnology). Proteins were visualized by using either secondary antibodies directly conjugated to Texas Red or the biotin/streptavidin-Texas Red-conjugated amplification method (GE Healthcare, Little Chalfont, Buckinghamshire, UK). Nuclei were labeled with Hoescht.

Cell Culture

VSMCs were isolated from the thoracic aorta of Syrian CHF 147 and WT hamsters and cultured as described elsewhere.[28] Proliferation was measured by using the CellTiter96 Cell Proliferation Assay kit (Promega, Charbonnières, France).

Single-Channel Recordings and Data Analysis

Experiments were performed with the cell-attached and/or inside-out patch-clamp configuration. Patch pipettes (10 to 15 mol/LΩ) were pulled from borosilicate glass capillaries (Corning Kovar Sealing 7052; WPI, Sarasota, FL). Currents were recorded with an Axopatch 200B amplifier (Axon Instruments, Foster City, CA). Channel activity (relative mean membrane patch current) was calculated as previously reported.[29] All experiments were conducted at room temperature (20 to 24°C). The superfusion control and bath solutions contained 128 mmol/L potassium aspartate, 2 mmol/L KCl, 1 mmol/L $BaCl_2$, 5 mmol/L ethylene glycol bis(β-aminoethyl ether)-N,N,N',N'-tetraacetic acid, 10 mmol/L HEPES, and 10 mmol/L glucose; pH was adjusted to 7.4 with KOH. The pipette solution contained 48 mmol/L $BaCl_2$ and 10 mmol/L HEPES; pH was adjusted to 7.4 with CsOH. When the patch pipette contained 48 mmol/L Ba^{2+}, and the patch membrane potential was continuously held at −80 mV (no voltage pulses being applied), spontaneous inward currents corresponding to channel opening were recorded. Ba^{2+} was used as charge carrier because it is generally considered that Ba^{2+} ions are more permeable than Ca^{2+} ions through several types of Ca^{2+} channels (L- and T-type), and this property seems to hold for B-type Ca^{2+} channels.[30] Because Ba^{2+} blocks practically all known K^+, Na^+, and Cl^- channels, it is useful for studying Ca^{2+} channels. We also wanted to avoid activating Ca^{2+}-activated K^+ or Cl^- channels by Ca^{2+} flowing through these channels. We used blockade by eosin applied to the internal face of the membrane patch to confirm the presence of B-type channels.

Confocal Microscopy

Slides were examined with a Zeiss LSM-510 laser scanning confocal microscope (Carl Zeiss GmbH,

Jena, Germany) equipped with a 30-mW argon laser and a 1-mW helium-neon laser, using a 20X/NA 0.75 Plan-Apochromat or 63X/NA 1.40 Plan Apochromat oil immersion objective. Green fluorescence was observed with a 505- to 550-nm band-pass emission filter under 488-nm laser illumination. Red fluorescence was observed with a 560-nm long-pass emission filter under 543-nm laser illumination. Pinholes were set at 1.0 Airy unit. Stacks of images were collected every 0.9 μm along the z axis. All settings were kept constant for reasons of comparability. Three median slices were projected for NFAT samples. For double immunofluorescence, dual excitation using the multitrack mode (images acquired sequentially) was obtained with the argon and He/Ne lasers.

Promoter Reporter Assay

Cells were transfected using FuGene 6 (Roche, Basel, Switzerland) with NFAT-promoter-luciferase construct (NFAT-Luc; Stratagene, Cambridge, UK). They were cultured for 48 hours without fetal calf serum (FCS) and then treated with 10% FCS alone or together with 5 μmol/L mibefradil or 10 μmol/L cyclosporine A (CsA) for 5 hours. The luciferase activity was measured by using "the luciferase assay kit" (Promega). It was expressed as percentage of control in relative luciferase units.

Mitochondrial Architecture and Activity

For live cell confocal microscopy, cells were plated on a collagen-coated coverglass chamber (Lab-Tek II Chamber 1.5 German Cover Glass System; Nalge Nunc International, Rochester, NY) and cultured in Dulbecco's modified Eagle's medium supplemented with 10% FCS for 24 to 48 hours. Then, the medium was replaced by Ham's F-12, with 25 mmol/L HEPES, without phenol red (Promocell, Heidelberg, Germany). To assess changes in mitochondrial membrane (Δ_m potential), live cells were double-labeled with the mitochondrion-sensitive Δ_m-independent probe MitoTracker Green (500 nmol/L, M7514; Invitrogen, Carlsbad, CA) and the Δ_m-sensitive dye MitoFluor Red (500 nmol/L, M22422; Invitrogen) according to manufacturers' instructions. Cells were observed in an inverted confocal microscope equipped with a chamber at 37°C. Fluorescence was recorded by means of confocal laser scanning microscopy (Leica TCS4D; Wetzlar, Germany) (λ_{ex}, 490 and 598 nm; λ_{em}, 516 and 630 nm, respectively).

Statistical Analysis

All quantitative data are means $\pm$ SEM of at least three independent experiments. An unpaired t-test was used to compare means. The nonparametric Mann-Whitney test was used to compare media thickness. Differences were considered significant when $P < 0.05$.

Results

Altered Phenotype of CHF 147 Thoracic Aorta VSMCs

In WT hamsters, media thickness was homogenous (Figure 1, A and C), whereas in CHF 147 hamsters, there were numerous zones of atrophy and marked hypertrophy (Figure 1B). One CHF 147 animal had global hypertrophy of the media, two had aspects similar to WT, and seven were globally atrophic. The mean CHF 147 value was lower than the WT value (15.8 $\pm$ 6.9 versus 19.4 $\pm$ 2.8 μm; $P < 0.001$).

To characterize the phenotype of CHF 147 VSMCs, aorta sections from six WT and six CHF 147 animals were labeled with antibodies specific for the contractile or synthetic phenotype and were then examined by immunofluorescence (Figure 2). The adult smooth muscle myosin heavy chain SM2 was present in aortic VSMCs from WT hamsters but was extensively replaced by the nonmuscular myosin heavy chain NM-B, a marker of the synthetic phenotype, in CHF 147 hamsters. Dystrophin, another marker of the contractile phenotype, was present in WT and absent in CHF 147 aortas, whereas caveolin-1, a specific marker of membrane caveolae, was expressed in both WT and myopathic animals.

Both SERCA 2a and RyR were present in the media of WT hamsters but absent from CHF 147 animals, as previously shown in proliferating VSMCs.[20,28] The other SERCA isoform, SERCA 2b, and the plasma membrane Ca^{2+} pump PMCA were present in both WT and CHF 147 animals. This suggested that CHF 147 VSMCs had a synthetic phenotype. Labeling with anti-cyclin D1, a marker of proliferation, confirmed the presence of proliferating cells in the media, and especially in the luminal part of the aorta, in five out of six CHF 147 animals studied; WT aortas were negative for cyclin D1 staining (Figure 2C). Cyclin D1 expression was variable along the aorta, with zones of strong expression and other zones of no expression. Thus, the CHF aorta displayed a heterogeneous pattern of undifferentiated/proliferating VSMCs. The apparent discrepancy between the proliferative phenotype of the VSMCs and the atrophic phenotype of the vessel might be due to apoptosis in the vessel wall (see VSMCs from CHF 147 Undergo Apoptosis).

Proliferative Properties of Isolated VSMCs

Freshly isolated VSMCs from WT hamsters expressed markers of the differentiated phenotype, such as SM2 and SERCA 2a, whereas these markers were absent from freshly isolated VSMCs from CHF 147 hamsters while NM-B MHC was present. Freshly dissociated VSMCs from CHF 147 hamsters resembled proliferating VSMCs from WT hamsters (Figure 3). When stimulated with serum (10%), the number of VSMCs in WT increased 4.5-fold after 2 days in culture, compared with less than twofold with VSMCs from CHF 147 hamsters cultured in the same conditions (Figure 4A).
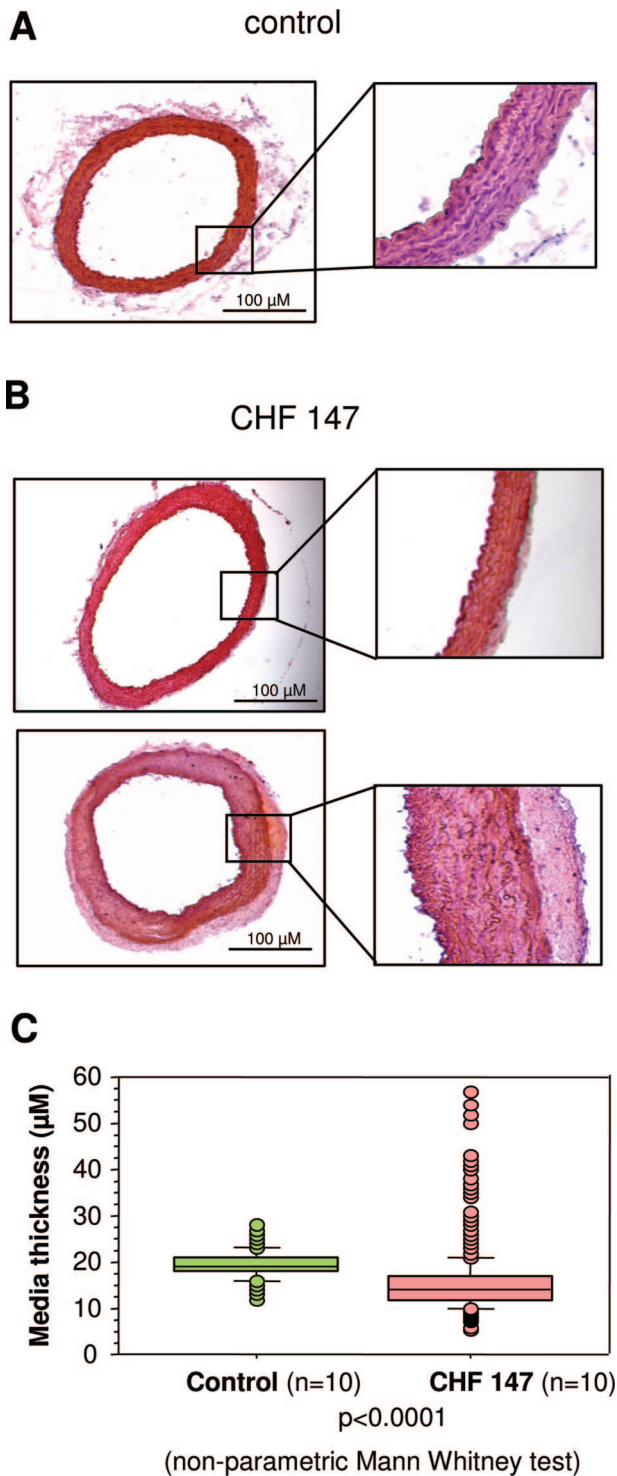
A   control

B   CHF 147

C

Figure 1. Morphometric analysis of the thoracic aorta from WT and cardiomyopathic (CHF 147) hamsters. Histological cross sections from WT (**A**) and CHF 147 hamsters (**B**) stained by hematoxylin-eosin are shown. The right panels are magnifications of the aortic wall. **C:** Distribution of media thickness.

Effect of Ca^{2+} Inhibitors on Proliferation

Increased plasma membrane permeability to Ca^{2+} has been described in cardiac and skeletal myocytes lacking δ-sarcoglycan.[8–11] In VSMCs, elevated cytosolic Ca^{2+}
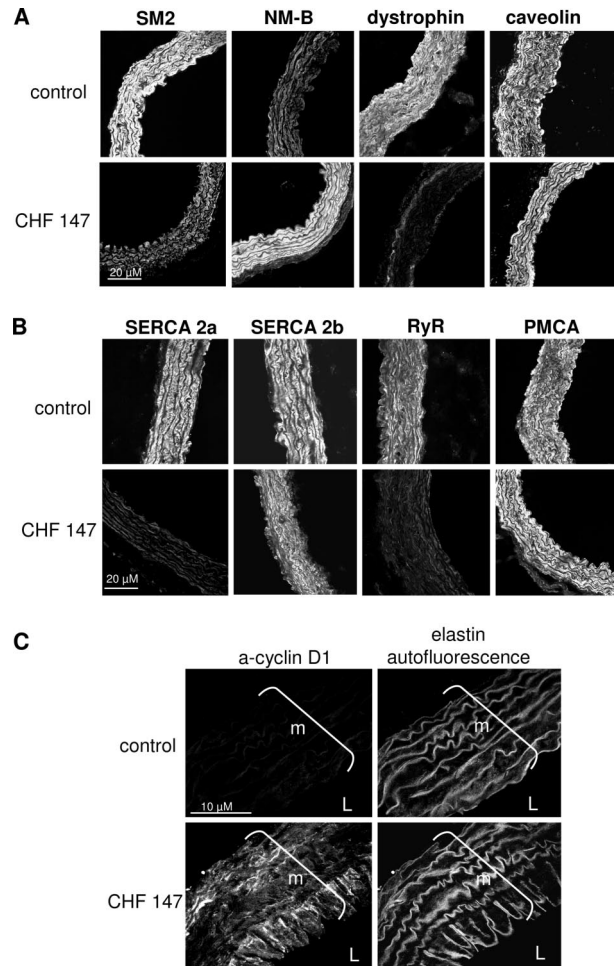

Figure 2. Phenotype of smooth muscle cells from thoracic aorta. Confocal immunofluorescence. **A:** Expression of markers of the synthetic phenotype: nonmuscular myosin heavy chain B (NM-B) and the contractile phenotype: smooth muscle myosin heavy chain 2 (SM2) and dystrophin. Expression of caveolin 1 is also shown. **B:** Expression of calcium-handling proteins: SERCA 2a, SERCA 2b, RyR, and PMCA. **C:** Expression of cyclin D1, a marker of cell proliferation. m, media; L, lumen.

levels induce proliferation and phenotypic changes.[21] We therefore tried to detect enhanced Ca^{2+} entry in CHF 147 VSMCs by using various Ca^{2+} inhibitors (Figure 4B). Diltiazem, an inhibitor of LTCC, had no effect on the proliferation of VSMCs from WT hamsters. Nifedipine, another LTCC inhibitor, prevented WT VSMC proliferation but only at a high concentration. Mibefradil, a putative T-type Ca^{2+} channel blocker, completely blocked VSMC proliferation when used at a low concentration (5 μmol/L). Carboxyamidotriazole and 2-aminoethoxydiphenyl borate, two nonspecific inhibitors of capacitative calcium entry, inhibited proliferation only partially and only at high concentrations. Because mibefradil most efficiently inhibited the proliferation of WT hamster VSMCs, we also tested its effect on serum-induced proliferation of CHF 147 VSMCs. As in WT, 5 μmol/L mibefradil completely inhibited the increase in cell numbers induced by serum. Because of the small amount of cells obtained from mutant hamsters, we were unable to test the other inhibitors. These results indicate that Ca^{2+} entry is involved in VSMC proliferation. The calcineurin inhibitor CsA partially
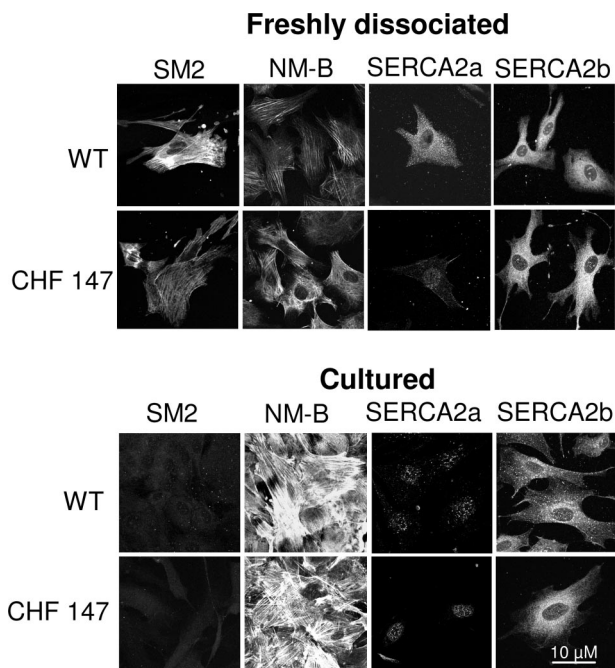
Freshly dissociated

Cultured

Figure 3. Characterization of primary VSMCs. **A:** Analysis of the phenotype of freshly dissociated or cultured (3 days, 10% FCS) VSMCs. Confocal immunofluorescence with specific antibodies to smooth muscle myosin heavy chain 2 (SM2), to the nonmuscle myosin heavy chain-B (NM-B), and to SERCA 2a and SERCA 2b is shown.

blocked the proliferation of VSMCs from WT hamsters (Figure 4B), suggesting the involvement of the calcium-dependent calcineurin/NFAT-signaling pathway in the proliferation of hamster VSMCs.

Analysis of B-Type Channels in VSMCs from Control and CHF 147 Hamsters: Effect of Mibefradil

To examine further the possibility of enhanced Ca^{2+} entry in CHF 147 VSMCs, we performed cell-attached and inside-out patch recordings using membranes of VSMCs freshly isolated from WT (Figure 5A) and CHF 147 hamsters (Figure 5B). In WT cells, single-channel activity (observed in 15% of membrane patches tested) exhibited rare bursts of intense activity followed by long-lasting quiescent periods. Channel activity, assessed as the relative mean patch current, was 0.030 ± 0.075 (mean $\pm$ SD, $n = 35$) (Figure 5E) in WT VSMCs. In contrast, in freshly isolated VSMCs from CHF 147 hamsters, spontaneous channel activity (35% of tested membrane patches) exhibited longer bursts of intense activity, separated by shorter quiescent periods (Figure 5B). The relative mean patch current was markedly enhanced to 0.45 ± 0.06 ($n = 24$) (Figure 5E) and was very similar to that observed in proliferating WT VSMCs (0.38 ± 0.09). Cultured CHF 147 VSMCs also showed marked channel activity (0.615 ± 0.10, $n = 27$) (Figure 5, D and E). The expanded-time scale trace designated "a" in Figure 5D shows the complex gating pattern of B-type channels, which was very similar to that previously observed with cardiac myocytes when B-type channel activity was in-
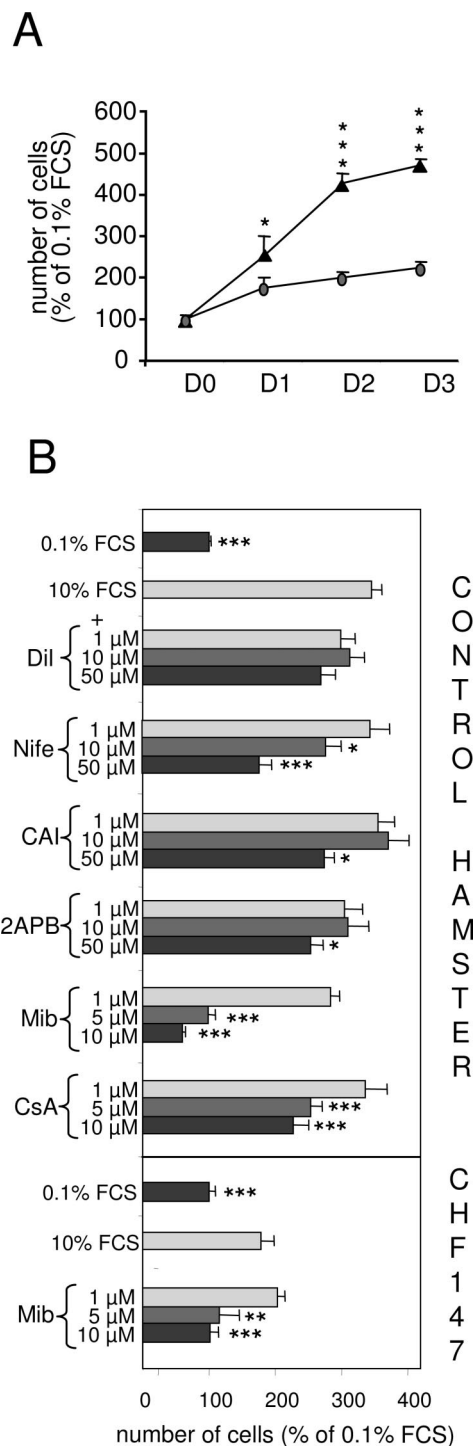

Figure 4. Proliferation of primary VSMCs in culture. **A:** Analysis of the growth capacity of VSMCs from WT (▲) and CHF 147 (●) in culture. Freshly isolated cells were cultured in the presence of serum (0.1 or 10%) for 24 to 72 hours. Each point represents the mean of three to five independent experiments. At each time point the number of cells was normalized to the number of cells in 0.1% FCS (control). Values are plotted as a percentage of the control value. *$P < 0.05$, ***$P < 0.01$ WT versus CHF 147 at the same time point. **B:** Pharmacological analysis of the calcium signaling pathways of serum-induced proliferation. VSMCs (passages 1 to 3) were cultured for 48 hours in the presence of 0.1 or 10% FCS, either alone (control) or together with drugs at the indicated concentrations. Dil, diltiazem; Nife, nifedipine; CAI, carboxyamidotriazole; 2APB, 2-aminoethoxydiphenyl borate; Mib, mibefradil. Data are expressed as a percentage of the cell number in control wells. The results represent the average of at least four independent experiments performed in tetraplicate. **$P < 0.05$, ***$P < 0.001$ versus control.
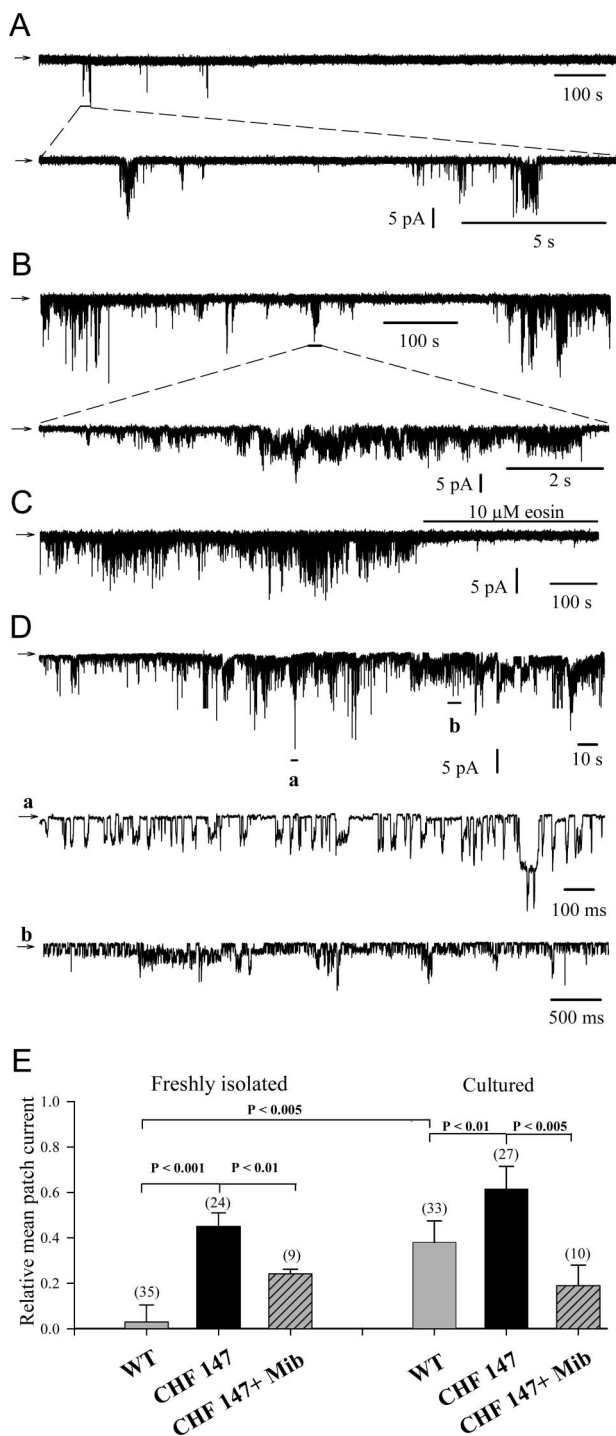
A

B

Figure 6. Involvement of NFAT in VSMC proliferation. **A:** Confocal immunofluorescence with anti-NFAT showing its cytosolic or nuclear localization in VSMCs. **B:** Promoter-reporter assay of NFAT transcriptional activity in WT VSMCs. Cells were transfected with NFAT-Luc and cultured for 48 hours without FCS. In **A** and **B**, cells were then treated with 10% FCS alone or together with 5 μmol/L mibefradil (Mib) or 10 μmol/L CsA for 5 hours. RLU, relative luminescence units. The bars represent mean ± SEM of three experiments in triplicate. ***$P < 0.001$ versus control (0.1% FCS).

Figure 5. B-type Ca^{2+} channel activity in primary VSMCs. B-type Ca^{2+} channel activity detected in membrane patches of freshly isolated WT VSMCs (**A**), freshly isolated CHF 147 VSMCs (**B**), cultured WT VSMCs (**C**), and cultured CHF 147 VSMCs (**D**). **E:** Bar graphs compare the relative mean patch current in experiments conducted as shown in **A–D**. The top traces are representative cell-attached recordings of spontaneous bursts of activity, showing the sporadic bursting nature of this channel activity obtained during application of control superfusion to the cell. The bottom traces are expanded time-scale extracts, as indicated. **Arrows** indicate zero current (closed level), and the downward deflexions are inwardly directed membrane currents. In **D**, bottom traces noted **a** and **b** are expanded time-scale extracts, as indicated. Numbers and bars denote the numbers of measurements obtained with different patches and corresponding SD value, respectively. *P* value was determined with Student's *t*-test. The membrane patch holding potential was −80 mV.
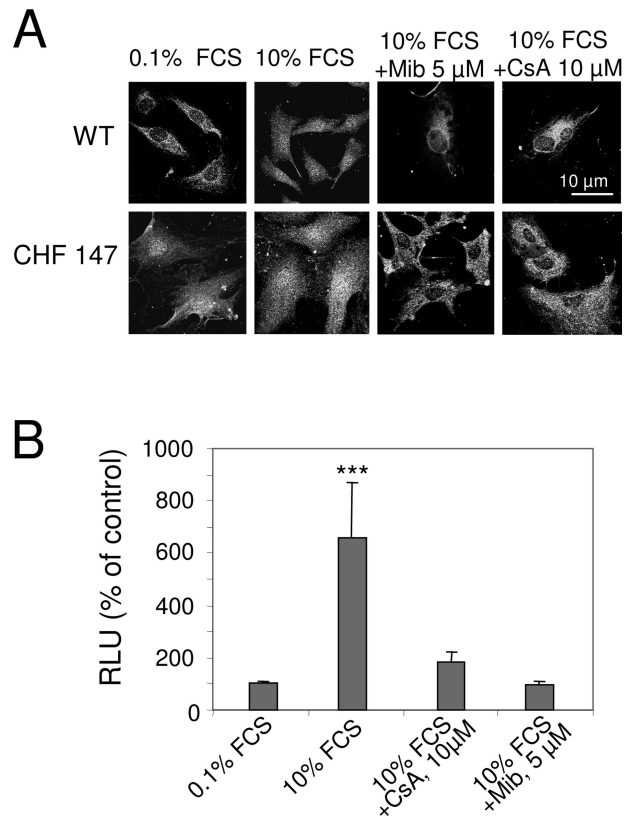
duced by chlorpromazine.[31] Eosin (10 μmol/L) completely blocked the channel activity (Figure 5C), an effect characteristic of B-type Ca^{2+} channels.[31] When channel recordings were made with mibefradil (20 μmol/L) in the pipette, channel activities in freshly isolated and cultured CHF 147 VSMCs were markedly reduced (to 0.24 ± 0.02 and 0.19 ± 0.02, respectively; Figure 5E).

Thus, freshly isolated VSMCs from CHF 147 possess voltage-independent basal Ca^{2+} channels with enhanced activity similar to that of proliferating WT cells. Mibefradil inhibited the activity of these channels.

NFAT Is Activated in CHF 147 VSMCs

The fact that cyclosporine A blocks proliferation suggests the participation of the calcineurin/NFAT pathway. In freshly isolated CHF 147 VSMCs, NFAT was already located in the nucleus (ie, activated), as in proliferating WT VSMCs. Serum stimulation had no effect on NFAT activity in CHF 147 VSMCs (Figure 6A). After treatment of WT VSMCs with mibefradil (5 μmol/L) or CsA (10 μmol/L) for 24 hours in the presence of 10% FCS, NFAT was arrested in the cytosol. Mibefradil and CsA also both inhibited the activity of an NFAT-driven luciferase construct transfected into WT VSMCs (Figure 6B). These data show that
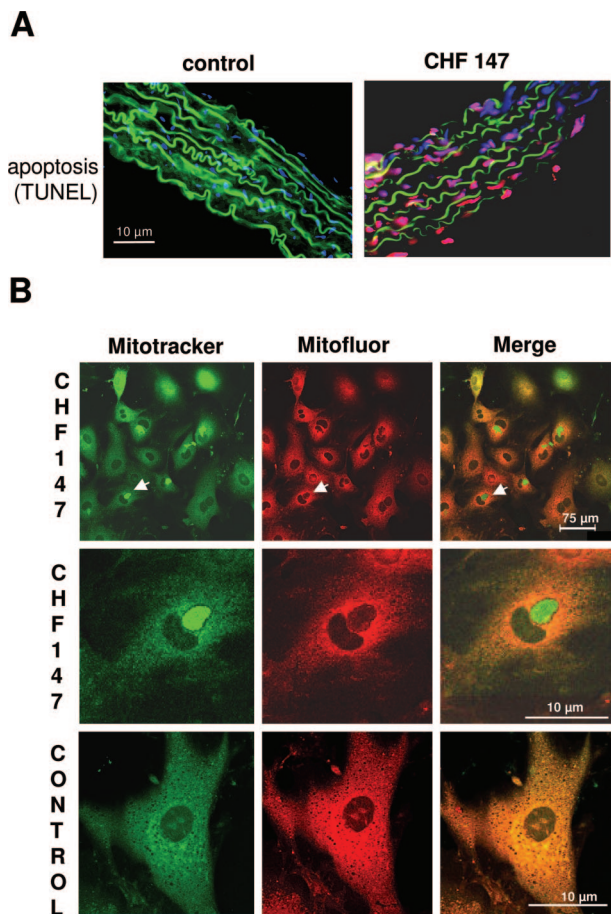
A

B

Figure 7. Apoptosis of CHF 147 VSMCs. **A:** Analysis of apoptosis in thoracic aorta cross-sections by the terminal deoxynucleotidyl transferase dUTP nick-end labeling method. The media are identified by elastin autofluorescence (green), apoptotic cells are terminal deoxynucleotidyl transferase dUTP nick-end labeling-positive (red), and nuclei are marked by Hoechst staining (blue). **B:** Mitochondrial aggregation in cultured CHF 147 VSMCs. Confocal microscopy of live cells double-immunolabeled with MitoTracker Green and MitoFluor Red was used to assess the mitochondrial architecture and mitochondrial membrane potential changes. The green and red images were superimposed to visualize mitochondria that had lost their Δ_m.

NFAT is spontaneously active in CHF 147 VSMCs and suggest the involvement of enhanced Ca^{2+} channel entry sensitive to mibefradil.

VSMCs from CHF 147 Undergo Apoptosis

The atrophic zones observed in the media of CHF147 aorta prompted us to screen for apoptotic cells with the terminal deoxynucleotidyl transferase dUTP nick-end labeling method. No apoptosis was observed in WT aortas, whereas CHF 147 aortas contained abundant apoptotic cells distributed in patches along the aorta (Figure 7A). The percentages of apoptotic cells in freshly dissociated CHF 147 and WT VSMCs were 29.7 ± 5.6 and $4.3 \pm 1.3\%$, respectively ($P < 0.05$). When cultured for 3 days with 10% serum, the proportion of apoptotic cells was $24.2 \pm 5.2\%$ in CHF 147 VSMCs and $1.7 \pm 1.7\%$ in WT VSMCs ($P < 0.05$).

Mitochondrial dysfunction is a major cause of apoptosis and is associated with cellular redistribution of mito-

chondria.[32] We used MitoTracker Green to locate mitochondria and MitoFluor Red to measure their membrane potential. Aggregation of mitochondria near the nucleus was observed in 25% of CHF 147 VSMCs but in no WT cells (Figure 7B, left panel). These mitochondria were not labeled with MitoFluor Red, indicating that they were inactive (Figure 7B, middle and right). Merge images showed the colocalization of MitoTracker Green and MitoFluor Red signals in WT cells, whereas in CHF 147 VSMCs, the red and green signals were superimposed in some cells but clearly distinct in others.

Discussion

We demonstrate that the δ-sarcoglycan deficiency in myopathic CHF 147 hamsters leads to peripheral vascular smooth muscle disorders characterized by anarchic proliferation and apoptosis. This vascular remodeling is associated with an increased transmembrane Ca^{2+} entry and with activation of a Ca^{2+}-dependent transcription pathway.

Vasospasm of small arteries such as coronary arteries is well documented in δ-sarcoglycan mutant animals,[5,33–35] but VSMC dysfunction is not the primary cause of δ-sarcoglycan-deficient muscular dystrophy.[2,36–38] Ca^{2+} channel blockers such as verapamil and mibefradil suppress vasospasm and improve cardiac function.[2,35,39–41] Here, we describe another vascular disorder in this genetic disease, characterized by media remodeling of large vessels.

Several arguments indicate that, in CHF 147 hamsters, VSMC proliferation is due to increased calcium entry. First, the Ca^{2+}-dependent calcineurin/NFAT-signaling pathway was activated as in control proliferating cells. Second, voltage-independent Ca^{2+} channel activity was markedly enhanced in VSMCs of δ-sarcoglycan-deficient animals and also in proliferating WT cells. These Ca^{2+} channels resemble basal Ca^{2+} channels described in cardiac myocytes (B-type channels), which are characterized by high conductance (>20 pS) and by their permeability to Ca^{2+} and Ba^{2+}. They are inhibited by La^{3+}, AlF_3, eosin, and, as shown here, by mibefradil, a drug that blocks several calcium channels, including Cav1.2 L-type Ca^{2+} channels[42,43] and store-operated channels.[44] Third, VSMC proliferation and NFAT translocation to the nucleus were both suppressed by mibefradil, suggesting a link between enhanced Ca^{2+} channel activity and phenotypic changes.

Mibefradil prevented VSMC proliferation *in vitro* and neointima formation in a carotid balloon injury model in rats.[45] It is unlikely that the antiproliferative effect of mibefradil is due to TTCC. TTCC were shown to control proliferation of human pulmonary myocytes,[46] but the absolute magnitude of whole-cell inward currents was small (5 ± 2 pA) compared with the currents measured in the present study. In addition, in our study Ca^{2+} entry was voltage-independent, whereas in Rodman's study the current was activated at -40 mV. Moreover, mibefradil inhibited TTCC expression and proliferation,[47] whereas functional voltage-gated TTCC could not be

detected in these tumor cell lines.[48] Thus, inhibition of proliferation by mibefradil was due to an effect independent of voltage-gated channels.[48] Furthermore, overexpression of TTCC generated by the human α_{1G} and α_{1H} subunits in human embryonic kidney 293 cells increased Ca^{2+} influx but not proliferation.[49]

Evidence of abnormal voltage-independent basal Ca^{2+} current in dystrophin-lacking skeletal muscle fibers has already been reported.[12] In this latter case, the current was attributed to SOC activation. Moreover, minidystrophin gene transfer normalizes SOC activity.[12] An increase in SOC activity has also been found during VSMC proliferation,[50,51] and inhibition by RNA silencing or by pharmacological agents (carboxyamidotriazole and 2-aminoethoxydiphenyl borate) strongly inhibits cell proliferation.[52] In our study, carboxyamidotriazole and 2-aminoethoxydiphenyl borate inhibited VSMC proliferation, but only at high concentrations (50 μmol/L) at which they are less specific for these channels. Moreover, SOC, which have very low conductance (24 fS to 2 pS) and which are regulated by submembrane calcium, cannot account for the strong channel activity recorded here in highly calcium-buffered proliferating hamster VSMCs. However, we cannot exclude the participation of other Ca^{2+} entry processes. Given that mibefradil can nonspecifically block multiple channels, the strong inhibition of mibefradil on proliferation of VSMCs could be due to additive effects on multiple channels. This is supported by the observation that, in our study, mibefradil only blocks half of the activity of B-type channels at a higher dose than used to almost fully block VSMC proliferation.

Resting VSMCs from rat cerebral arteries show nearly continual Ca^{2+} influx, called "Ca^{2+} sparklets" due to the opening of single or clustered L-type Ca^{2+} channels in a voltage-independent manner at resting potential.[53,54] It is unlikely that LTCC contribute significantly to the strong channel activity in CHF 147 VSMCs. Moreover, diltiazem or nifedipine had little effect on VSMC proliferation, in keeping with the absence of LTCC in proliferating cells.[55–57] However, similarly to the data of Santana group,[53,54] our results point to the role of calcium channel bursts in the regulation of calcium-dependent processes in VSMCs.

One major finding of this study is that increased mibefradil-sensitive Ca^{2+} entry is coupled to the transcription factor NFAT pathway in freshly isolated CHF 147 and WT VSMCs. Increased calcineurin/PP2B and NFAT activity has also been detected in ventricular myocytes from δ-sarcoglycan-deficient J2N-k and UM-X7.1 cardiomyopathic hamsters.[58,59] NFAT is strongly required for VSMC proliferation. Indeed, NFATc3 is activated in rat VSMCs *in vitro* by agonists that lead to proliferation[28,60–63] and after balloon-induced restenosis *in vivo*.[24,25] Forced expression of the NFAT-competing peptide VIVIT blocked VSMC proliferation both *in vitro* and *in vivo*.[24,62] Finally, NFAT is involved in the control of cyclin D1 and pRb, and its inhibition leads to cell cycle arrest in the G_1 phase[24]

We also observed abundant apoptosis in the vascular wall of CHF 147 hamsters, accompanied by mitochondrial abnormalities. Apoptosis and mitochondrial dysfunction have been observed in several models of myopathies, such as γ-sarcoglycan-deficient mice,[64] desmin-related cardiomyopathy,[65] and collagen deficiency-related myopathy.[66] An important feature of the mitochondrial dysfunction observed here in CHF 147 VSMCs is their redistribution and aggregation around the nucleus, possibly representing an early step of apoptosis.[32,67] Mitochondria are dynamic organelles and their movements result in spatial rearrangement of ATP production and Ca^{2+} buffering. For instance, elevation of the global $[Ca^{2+}]_c$ to 1 μmol/L results in almost complete loss of mitochondrial movement.[68] An increase in mitochondrial Ca^{2+} is observed in dystrophin-lacking myocytes,[12,69] whereas lowering calcium entry by minidystrophin expression results in shorter calcium transients and reduced calcium uptake by mitochondria.[12] We have no evidence of a link between enhanced voltage-independent channel activity, mitochondria calcium loading and apoptosis. However, we have previously shown that B-type Ca^{2+} channels can modulate mitochondrial calcium loading during cardiac myocyte apoptosis induced by ceramide.[70] The fact that both proliferation and apoptosis are observed in the same vessel suggests that the aortic vessel wall is able to regenerate at the difference of the myocardium.

In conclusion, we demonstrate that the mutation of a cytoskeleton protein affects the activity of voltage-independent Ca^{2+} channels and triggers the activation of Ca^{2+} signaling pathways in vascular smooth muscle cells, resulting in major changes in phenotype and survival. Such a mechanism may not be restricted to sarcoglycanopathy but may concern other diseases characterized by dystrophin disruption and sarcolemma instability such as heart failure.[71]

References

1. Tsubata S, Bowles KR, Vatta M, Zintz C, Titus J, Muhonen L, Bowles NE, Towbin JA: Mutations in the human delta-sarcoglycan gene in familial and sporadic dilated cardiomyopathy. J Clin Invest 2000, 106:655–662
2. Wheeler MT, Korcarz CE, Collins KA, Lapidos KA, Hack AA, Lyons MR, Zarnegar S, Earley JU, Lang RM, McNally EM: Secondary coronary artery vasospasm promotes cardiomyopathy progression. Am J Pathol 2004, 164:1063–1071
3. Sakamoto A, Ono K, Abe M, Jasmin G, Eki T, Murakami Y, Masaki T, Toyo-oka T, Hanaoka F: Both hypertrophic and dilated cardiomyopathies are caused by mutation of the same gene, delta-sarcoglycan, in hamster: an animal model of disrupted dystrophin-associated glycoprotein complex. Proc Natl Acad Sci USA 1997, 94:13873–13878
4. Hack AA, Cordier L, Shoturma DI, Lam MY, Sweeney HL, McNally EM: Muscle degeneration without mechanical injury in sarcoglycan deficiency. Proc Natl Acad Sci USA 1999, 96:10723–10728
5. Coral-Vazquez R, Cohn RD, Moore SA, Hill JA, Weiss RM, Davisson RL, Straub V, Barresi R, Bansal D, Hrstka RF, Williamson R, Campbell KP: Disruption of the sarcoglycan-sarcospan complex in vascular smooth muscle: a novel mechanism for cardiomyopathy and muscular dystrophy. Cell 1999, 98:465–474
6. Miyata S, Takemura G, Li Y, Okada H, Maruyama R, Ushikoshi H, Esaki M, Kanamori H, Li L, Misao Y, Tezuka A, Toyo-Oka T, Minatoguchi S, Fujiwara T, Fujiwara H: Autophagic cardiomyocyte death in cardiomyopathic hamsters and its prevention by granulocyte colony-stimulating factor. Am J Pathol 2006, 168:386–397
7. Wheeler MT, McNally EM: Sarcoglycans in vascular smooth and striated muscle. Trends Cardiovasc Med 2003, 13:238–243

8. Turner PR, Fong PY, Denetclaw WF, Steinhardt RA: Increased calcium influx in dystrophic muscle. J Cell Biol 1991, 115:1701–1712

9. Fong PY, Turner PR, Denetclaw WF, Steinhardt RA: Increased activity of calcium leak channels in myotubes of Duchenne human and mdx mouse origin. Science 1990, 250:673–676

10. Iwata Y, Katanosaka Y, Arai Y, Komamura K, Miyatake K, Shigekawa M: A novel mechanism of myocyte degeneration involving the Ca^{2+}-permeable growth factor-regulated channel. J Cell Biol 2003, 161:957–967

11. Tutdibi O, Brinkmeier H, Rudel R, Fohr KJ: Increased calcium entry into dystrophin-deficient muscle fibres of MDX and ADR-MDX mice is reduced by ion channel blockers. J Physiol 1999, 515:859–868

12. Vandebrouck A, Ducret T, Basset O, Sebille S, Raymond G, Ruegg U, Gailly P, Cognard C, Constantin B: Regulation of store-operated calcium entries and mitochondrial uptake by minidystrophin expression in cultured myotubes. FASEB J 2006, 20:136–138

13. Vandebrouck C, Martin D, Colson-Van Schoor M, Debaix H, Gailly P: Involvement of TRPC in the abnormal calcium influx observed in dystrophic (mdx) mouse skeletal muscle fibers. J Cell Biol 2002, 158:1089–1096

14. Johnson BD, Scheuer T, Catterall WA: Convergent regulation of skeletal muscle Ca2+ channels by dystrophin, the actin cytoskeleton, and cAMP-dependent protein kinase. Proc Natl Acad Sci USA 2005, 102:4191–4196

15. Nakamura TY, Iwata Y, Sampaolesi M, Hanada H, Saito N, Artman M, Coetzee WA, Shigekawa M: Stretch-activated cation channels in skeletal muscle myotubes from sarcoglycan-deficient hamsters. Am J Physiol 2001, 281:C690–C699

16. Vandebrouck A, Sabourin J, Rivet J, Balghi H, Sebille S, Kitzis A, Raymond G, Cognard C, Bourmeyster N, Constantin B: Regulation of capacitative calcium entries by alpha1-syntrophin: association of TRPC1 with dystrophin complex and the PDZ domain of alpha1-syntrophin. FASEB J 2007, 21:608–617

17. Marchand E, Constantin B, Balghi H, Claudepierre MC, Cantereau A, Magaud C, Mouzou A, Raymond G, Braun S, Cognard C: Improvement of calcium handling and changes in calcium-release properties after mini- or full-length dystrophin forced expression in cultured skeletal myotubes. Exp Cell Res 2004, 297:363–379

18. Friedrich O, Both M, Gillis JM, Chamberlain JS, Fink RH: Mini-dystrophin restores L-type calcium currents in skeletal muscle of transgenic mdx mice. J Physiol 2004, 555:251–265

19. Quignard JF, Harricane MC, Menard C, Lory P, Nargeot J, Capron L, Mornet D, Richard S: Transient down-regulation of L-type Ca(2+) channel and dystrophin expression after balloon injury in rat aortic cells. Cardiovasc Res 2001, 49:177–188

20. Vallot O, Combettes L, Jourdon P, Inamo J, Marty I, Claret M, Lompre AM: Intracellular Ca(2+) handling in vascular smooth muscle cells is affected by proliferation. Arterioscler Thromb Vasc Biol 2000, 20:1225–1235

21. Lipskaia L, Lompré AM: Alteration in temporal kinetics of Ca2+ signaling and control of growth and proliferation. Biol Cell 2004, 96:55–68

22. Bading H, Ginty DD, Greenberg ME: Regulation of gene expression in hippocampal neurons by distinct calcium signaling pathways. Science 1993, 260:181–186

23. Dolmetsch RE, Lewis RS, Goodnow CC, Healy JI: Differential activation of transcription factors induced by Ca2+ response amplitude and duration. Nature 1997, 386:855–858

24. Lipskaia L, del Monte F, Capiod T, Yacoubi S, Hadri L, Hours M, Hajjar RJ, Lompre AM: Sarco/endoplasmic reticulum Ca2+-ATPase gene transfer reduces vascular smooth muscle cell proliferation and neointima formation in the rat. Circ Res 2005, 97:488–495

25. Liu Z, Zhang C, Dronadula N, Li Q, Rao GN: Blockade of nuclear factor of activated T cells activation signaling suppresses balloon injury-induced neointima formation in a rat carotid artery model. J Biol Chem 2005, 280:14700–14708

26. Eggermont JA, Wuytack F, Verbist J, Casteels R: Expression of endoplasmic-reticulum Ca2(+)-pump isoforms and of phospholamban in pig smooth-muscle tissues. Biochem J 1990, 271:649–653

27. Marty I, Robert M, Villaz M, De Jongh K, Lai Y, Catterall WA, Ronjat M: Biochemical evidence for a complex involving dihydropyridine receptor and ryanodine receptor in triad junctions of skeletal muscle. Proc Natl Acad Sci USA 1994, 91:2270–2274

28. Lipskaia L, Pourci ML, Delomenie C, Combettes L, Goudouneche D, Paul JL, Capiod T, Lompre AM: Phosphatidylinositol 3-kinase and calcium-activated transcription pathways are required for VLDL-induced smooth muscle cell proliferation. Circ Res 2003, 92:1115–1122

29. Coulombe A, Lefevre IA, Baro I, Coraboeuf E: Barium- and calcium-permeable channels open at negative membrane potentials in rat ventricular myocytes. J Membr Biol 1989, 111:57–67

30. Lefevre T, Coraboeuf E, Ghazi A, Coulombe A: Divalent cation channels activated by phenothiazines in membrane of rat ventricular myocytes. J Membr Biol 1995, 147:147–158

31. Antoine S, Pinet C, Coulombe A: Are B-type Ca^{2+} channels of cardiac myocytes akin to the passive ion channel in the plasma membrane Ca^{2+} pump? J Membr Biol 2001, 179:37–50

32. Desagher S, Martinou JC: Mitochondria as the central control point of apoptosis. Trends Cell Biol 2000, 10:369–377

33. Factor SM, Minase T, Cho S, Dominitz R, Sonnenblick EH: Microvascular spasm in the cardiomyopathic Syrian hamster: a preventable cause of focal myocardial necrosis. Circulation 1982, 66:342–354

34. Sonnenblick EH, Fein F, Capasso JM, Factor SM: Microvascular spasm as a cause of cardiomyopathies and the calcium-blocking agent verapamil as potential primary therapy. Am J Cardiol 1985, 55:179B–184B

35. Cohn RD, Durbeej M, Moore SA, Coral-Vazquez R, Prouty S, Campbell KP: Prevention of cardiomyopathy in mouse models lacking the smooth muscle sarcoglycan-sarcospan complex. J Clin Invest 2001, 107:R1–7

36. Durbeej M, Sawatzki SM, Barresi R, Schmainda KM, Allamand V, Michele DE, Campbell KP: Gene transfer establishes primacy of striated vs. smooth muscle sarcoglycan complex in limb-girdle muscular dystrophy. Proc Natl Acad Sci USA 2003, 100:8910–8915

37. Wheeler MT, Allikian MJ, Heydemann A, Hadhazy M, Zarnegar S, McNally EM: Smooth muscle cell-extrinsic vascular spasm arises from cardiomyocyte degeneration in sarcoglycan-deficient cardiomyopathy. J Clin Invest 2004, 113:668–675

38. Kawada T, Nakazawa M, Nakauchi S, Yamazaki K, Shimamoto R, Urabe M, Nakata J, Hemmi C, Masui F, Nakajima T, Suzuki J, Monahan J, Sato H, Masaki T, Ozawa K, Toyo-Oka T: Rescue of hereditary form of dilated cardiomyopathy by rAAV-mediated somatic gene therapy: amelioration of morphological findings, sarcolemmal permeability, cardiac performances, and the prognosis of TO-2 hamsters. Proc Natl Acad Sci USA 2002, 99:901–906

39. Kumamoto H, Okamoto H, Watanabe M, Onozuka H, Yoneya K, Nakagawa I, Chiba S, Watanabe S, Mikami T, Abe K, Kitabatake A: Beneficial effect of myocardial angiogenesis on cardiac remodeling process by amlodipine and MCI-154. Am J Physiol 1999, 276:H1117–H1123

40. Villame J, Massicotte J, Jasmin G, Dumont L: Effects of mibefradil, a T- and L-type calcium channel blocker, on cardiac remodeling in the UM-X7.1 cardiomyopathic hamster. Cardiovasc Drugs Ther 2001, 15:41–48

41. Paquette F, Jasmin G, Dumont L: Cardioprotective efficacy of verapamil and mibefradil in young UM-X7.1 cardiomyopathic hamsters. Cardiovasc Drugs Ther 1999, 13:525–530

42. Leuranguer V, Mangoni ME, Nargeot J, Richard S: Inhibition of T-type and L-type calcium channels by mibefradil: physiologic and pharmacologic bases of cardiovascular effects. J Cardiovasc Pharmacol 2001, 37:649–661

43. Moosmang S, Haider N, Bruderl B, Welling A, Hofmann F: Antihypertensive effects of the putative T-type calcium channel antagonist mibefradil are mediated by the L-type calcium channel Cav1.2. Circ Res 2006, 98:105–110

44. Gackière F, Bidaux G, Lory P, Prevarskaya N, Mariot P: A role for voltage gated T-type calcium channels in mediating "capacitative" calcium entry? Cell Calcium 2006, 39:357–366

45. Schmitt R, Clozel JP, Iberg N, Buhler FR: Mibefradil prevents neointima formation after vascular injury in rats. Possible role of the blockade of the T-type voltage-operated calcium channel. Arterioscler Thromb Vasc Biol 1995, 15:1161–1165

46. Rodman DM, Reese K, Harral J, Fouty B, Wu S, West J, Hoedt-Miller M, Tada Y, Li KX, Cool C, Fagan K, Cribbs L: Low-voltage-activated (T-type) calcium channels control proliferation of human pulmonary artery myocytes. Circ Res 2005, 96:864–872

47. Panner A, Cribbs LL, Zainelli GM, Origitano TC, Singh S, Wurster RD: Variation of T-type calcium channel protein expression affects cell division of cultured tumor cells. Cell Calcium 2005, 37:105–119

48. Lu F, Chen H, Zhou C, Wu S: Is there a role for T-type Ca^{2+} channel in glioma cell proliferation? Cell Calcium 2005, 38:593–595; author reply 597

49. Chemin J, Monteil A, Briquaire C, Richard S, Perez-Reyes E, Nargeot J, Lory P: Overexpression of T-type calcium channels in HEK-293 cells increases intracellular calcium without affecting cellular proliferation. FEBS Lett 2000, 478:166–172

50. Golovina VA: Cell proliferation is associated with enhanced capacitative Ca(2+) entry in human arterial myocytes. Am J Physiol 1999, 277:C343–C349

51. Golovina VA, Platoshyn O, Bailey CL, Wang J, Limsuwan A, Sweeney M, Rubin LJ, Yuan JX: Upregulated TRP and enhanced capacitative Ca(2+) entry in human pulmonary artery myocytes during proliferation. Am J Physiol 2001, 280:H746–H755

52. Mignen O, Brink C, Enfissi A, Nadkarni A, Shuttleworth TJ, Giovannucci DR, Capiod T: Carboxyamidotriazole-induced inhibition of mitochondrial calcium import blocks capacitative calcium entry and cell proliferation in HEK-293 cells. J Cell Sci 2005, 118:5615–5623

53. Navedo MF, Amberg GC, Nieves M, Molkentin JD, Santana LF: Mechanisms underlying heterogeneous Ca^{2+} sparklet activity in arterial smooth muscle. J Gen Physiol 2006, 127:611–622

54. Navedo MF, Amberg GC, Votaw VS, Santana LF: Constitutively active L-type Ca^{2+} channels. Proc Natl Acad Sci USA 2005, 102:11112–11117

55. Gollasch M, Haase H, Ried C, Lindschau C, Morano I, Luft FC, Haller H: L-type calcium channel expression depends on the differentiated state of vascular smooth muscle cells. FASEB J 1998, 12:593–601

56. Kuga T, Kobayashi S, Hirakawa Y, Kanaide H, Takeshita A: Cell cycle-dependent expression of L- and T-type Ca^{2+} currents in rat aortic smooth muscle cells in primary culture. Circ Res 1996, 79:14–19

57. Richard S, Neveu D, Carnac G, Bodin P, Travo P, Nargeot J: Differential expression of voltage-gated Ca(2+)-currents in cultivated aortic myocytes. Biochim Biophys Acta 1992, 1160:95–104

58. Mitsuhashi S, Saito N, Watano K, Igarashi K, Tagami S, Shima H, Kikuchi K: Defect of delta-sarcoglycan gene is responsible for development of dilated cardiomyopathy of a novel hamster strain, J2N-k: calcineurin/PP2B activity in the heart of J2N-k hamster. J Biochem (Tokyo) 2003, 134:269–276

59. Ambra R, Di Nardo P, Fantini C, Minieri M, Canali R, Natella F, Virgili F: Selective changes in DNA binding activity of transcription factors in UM-X7.1 cardiomyopathic hamsters. Life Sci 2002, 71:2369–2381

60. Stevenson AS, Gomez MF, Hill-Eubanks DC, Nelson MT: NFAT4 movement in native smooth muscle. A role for differential Ca^{2+} signaling. J Biol Chem 2001, 276:15018–15024

61. Suzuki E, Nishimatsu H, Satonaka H, Walsh K, Goto A, Omata M, Fujita T, Nagai R, Hirata Y: Angiotensin II induces myocyte enhancer factor 2- and calcineurin/nuclear factor of activated T cell-dependent transcriptional activation in vascular myocytes. Circ Res 2002, 90:1004–1011

62. Yellaturu CR, Ghosh SK, Rao RK, Jennings LK, Hassid A, Rao GN: A potential role for nuclear factor of activated T-cells in receptor tyrosine kinase and G-protein-coupled receptor agonist-induced cell proliferation. Biochem J 2002, 368:183–190

63. Gomez MF, Stevenson AS, Bonev AD, Hill-Eubanks DC, Nelson MT: Opposing actions of inositol 1,4,5-trisphosphate and ryanodine receptors on nuclear factor of activated T-cells regulation in smooth muscle. J Biol Chem 2002, 277:37756–37764

64. Hack AA, Ly CT, Jiang F, Clendenin CJ, Sigrist KS, Wollmann RL, McNally EM: γ-Sarcoglycan deficiency leads to muscle membrane defects and apoptosis independent of dystrophin. J Cell Biol 1998, 142:1279–1287

65. Maloyan A, Sanbe A, Osinska H, Westfall M, Robinson D, Imahashi K, Murphy E, Robbins J: Mitochondrial dysfunction and apoptosis underlie the pathogenic process in alpha-B-crystallin desmin-related cardiomyopathy. Circulation 2005, 112:3451–3461

66. Irwin WA, Bergamin N, Sabatelli P, Reggiani C, Megighian A, Merlini L, Braghetta P, Columbaro M, Volpin D, Bressan GM, Bernardi P, Bonaldo P: Mitochondrial dysfunction and apoptosis in myopathic mice with collagen VI deficiency. Nat Genet 2003, 35:367–371

67. Haga N, Fujita N, Tsuruo T: Mitochondrial aggregation precedes cytochrome c release from mitochondria during apoptosis. Oncogene 2003, 22:5579–5585

68. Yi M, Weaver D, Hajnoczky G: Control of mitochondrial motility and distribution by the calcium signal: a homeostatic circuit. J Cell Biol 2004, 167:661–672

69. Robert V, Massimino ML, Tosello V, Marsault R, Cantini M, Sorrentino V, Pozzan T: Alteration in calcium handling at the subcellular level in mdx myotubes. J Biol Chem 2001, 276:4647–4651

70. Hénaff M, Antoine S, Mercadier JJ, Coulombe A, Hatem SN: The voltage-independent B-type Ca^{2+} channel modulates apoptosis of cardiac myocytes. FASEB J 2002, 16:99–101

71. Toyo-Oka T, Kawada T, Nakata J, Xie H, Urabe M, Masui F, Ebisawa T, Tezuka A, Iwasawa K, Nakajima T, Uehara Y, Kumagai H, Kostin S, Schaper J, Nakazawa M, Ozawa K: Translocation and cleavage of myocardial dystrophin as a common pathway to advanced heart failure: a scheme for the progression of cardiac dysfunction. Proc Natl Acad Sci USA 2004, 101:7381–7385